Bull. Mater. Sci., Vol. 34, No. 3, June 2011, pp. 447–454. © Indian Academy of Sciences.

An investigation in $InGaO_3(ZnO)_m$ pellets as cause of variability in thin film transistor characteristics

SONACHAND ADHIKARI[†], RAJEEV GUPTA[†,††], ASHISH GARG[†††] and DEEPAK[†††,*]

[†]Materials Science Programme, [††]Department of Physics, [†††]Department of Materials Science and Engineering and Samtel Centre for Display Technologies, Indian Institute of Technology, Kanpur 208 016, India

MS received 27 September 2010

Abstract. Indium–gallium–zinc oxide (IGZO) is a novel amorphous oxide semiconductor, which recently has received much attention for thin film transistors (TFTs) in flat panel displays. Published literature reports significant variations in the properties of thin films and TFTs prepared from IGZO even though the reported process conditions are similar. We demonstrate that these differences could arise from the method for preparation of targets from which the films are made. Accordingly, we also propose simple and appropriate conditions, specifically using much lower sintering temperatures and thus avoiding use of sealed Pt tubes for preparation of IGZO targets in composition range, $InGaO_3(ZnO)_m$, with $1 \leq m \leq 5$. These target materials are suitable in physical vapour deposition processes such as pulsed laser deposition and sputtering. In developing the process for sintering, the phase analysis of the target pellets was carried out using X-ray diffraction (XRD). The chemical compositions of the phases are also confirmed with inductively coupled plasma optical emission spectrometry (ICP-OES) and energy dispersive X-ray (EDX) techniques. We also demonstrate successful deposition of amorphous IGZO thin films by pulse laser deposition using the targets prepared by the proposed sintering process. Finally, we demonstrate that unmonitored method of making pellets for films deposition is a cause of variability associated in published literature on IGZO TFTs.

Keywords. IGZO; pellet; sintering.

1. Introduction

Indium–gallium–zinc oxide (IGZO) is currently an extensively researched material for application in thin film transistors (TFTs). IGZO was first synthesized by Kimizuka and Mohri (1985), then Orita *et al* (2001) reported first thin films of IGZO prepared using excimer pulsed laser deposition (PLD). These reports fuelled further research on IGZO owing to its promise in many technological applications. For instance, TFTs based on IGZO have been prepared by sputtering, PLD and sol–gel (Kim *et al* 2008; Koo *et al* 2008) techniques for fabricating active matrix liquid crystal display (AMLCD) and active matrix organic light emitting diode (AMOLED) display prototypes driven by IGZO TFTs (Lee *et al* 2007; Jeong *et al* 2008; Lee *et al* 2008).

1.1 *TFTs of IGZO*

Nomura *et al* (2003) investigated the electrical properties with respect to carrier concentration, hall mobility, field effect mobility and conductivity in single crystalline $InGaO_3(ZnO)_m$ with varying values of m. Their results show that the conductivity increases with an increase in m, ultimately saturating for $m > 40$. Correspondingly, the hall and field effect mobility also increase with increasing m, with hall mobility always greater than the field mobility. PLD method was used to deposit these films and, as in most published literature, it is not clear how the target was prepared. But, in order to compare the performance of IGZO based TFTs reported in the literature, it is important to ensure that the composition of target IGZO is completely replicated in thin films of IGZO, which cannot be ascertained in the absence of any data.

In TFTs with IGZO as the active layer, we have observed considerable variation in the properties of TFTs. Results are reported in table 1 for the composition of $InGaZnO_4$ deposited by PLD. The parameters of interest are field effect mobility, threshold voltage, on-off ratio, sub-threshold voltage swing and the materials used. We notice that the on-off current ratio (I_{ON}:I_{OFF}) of TFT varies from 10^3 (Nomura *et al* 2004) to 10^6 (Nomura *et al* 2006; Hosono 2006) for the TFT fabricated with similar substrate, gate, insulator and electrode materials. This variation could have its origin in IGZO film conductivity or the quality of the insulator. Similarly, the variation in the field effect mobility of TFT changes from <1 to 7 cm^2/Vs for the same carrier concentration, as the laser fluence increases from 2 to 9 J/cm^2. This variation in field effect mobility is consistent with the changes in hall mobility of the thin films from 0·9 to 9 cm^2/Vs (Hosono *et al* 2008). IGZO TFT with the active material deposited by PLD at 5·2 Pa showed a depletion mode TFT with a threshold

*Author for correspondence (saboo@iitk.ac.in)

Table 1. Values of field effect mobility (μ_{FE}), threshold voltage (V_{th}), I_{ON}/I_{OFF} ratio and sub-threshold voltage swing of TFTs in which IGZO of composition $InGaO_3(ZnO)_1$ was deposited by PLD.

Sl. No.	μ_{FE} (cm^2/V.s)	V_{th} (V)	I_{ON}/I_{OFF}	S. Swing (V/decade)	Substrate, gate, insulator, source and drain	Comment	Reference
1	5·6	∼+1·6	10^3		PET, ITO,Y_2O_3, ITO		Nomura *et al* (2004)
2	9	+1·3	10^6	0·24	PET, ITO, Y_2O_3, ITO		Nomura *et al* (2006)
3	12		$>10^6$	0·2	PET, ITO, Y_2O_3, ITO		Hosono (2006)
4	<1, 7			>1, 0·2	Si, Si, SiO_2, Au/ITO	For fluence of 2 and 9 J/cm^2	Hosono *et al* (2008)
5	9·19, 7·84	−6·54, +0·49	$>10^6$, $>10^6$	0·224, 0·104	Si, Si, SiO_2, ITO	For P_{O2} of 5·2 and 6·5 Pa	Hsieh *et al* (2008)
6	5·8	+6·2	2×10^5		Si, Si, BST, Ti/Au	For P_{O2} of 5 Pa	Yuan *et al* (2009)

Table 2. Carrier concentration, resistivity and Hall mobility data of $InGaOZnO_4$ thin films deposited by PLD.

P_{O2} (Pa)	T_{sub} (°C)	n (cm^{-3})	ρ (Ω cm)	μ_H ($cm^2\ V^{-1}\ s^{-1}$)	Fluence (Jcm^{-2})	Substrate	Reference
0·05	*RT*	$1·5 \times 10^{14}$	$7·5 \times 10^3$	3·9	1·5	Fused Silica	Yuan *et al* (2009)
0·1	*RT*	10^{20}	–	–	1·5–3	Corning #1737	Takagi *et al* (2005)
0·1	*RT*	5×10^{14}	10^3	3·3	1·5	Fused Silica	Yuan *et al* (2009)
0·25	110	10^{19}	5×10^{-2}	–	1·67	Corning #1737	Inoue *et al* (2008)
0·5	*RT*	$1·7 \times 10^{15}$	10^3	1	1·5	Fused Silica	Yuan *et al* (2009)
0·8	*RT*	$7·7 \times 10^{19}$	$3·85 \times 10^{-3}$	21	4–6	SiO_2	Orita *et al* (2001)
1	*RT*	7×10^{19}	$5·95 \times 10^{-3}$	15	–	Glass	Nomura *et al* (2006); Hosono (2006); Kamiya *et al* (2006)
1	*RT*	3–5 $\times 10^{19}$	$6·25 \times 10^{-2}$	2·5	2	SiO_2 glass	Hosono *et al* (2008); Nomura *et al* (2008a, b)
1	*RT*	3–5 $\times 10^{19}$	$1·04 \times 10^{-2}$	15	9	SiO_2 glass	Hosono *et al* (2008); Nomura *et al* (2008a, b)
1	*RT*	5×10^{19}	–	–	5	Corning #1737	Shimura *et al* (2008)
1	*RT*	$4·5 \times 10^{14}$	10^3	0·9	1·5	Fused Silica	Yuan *et al* (2009)
3	*RT*	$7·0 \times 10^{19}$	$4·55 \times 10^{-2}$	2	1·3	SiO_2 glass	Ohta *et al* (2008)
4	*RT*	7×10^{17}	–	–	5	Corning #1737	Shimura *et al* (2008)
5	*RT*	$4·7 \times 10^{13}$	$1·1 \times 10^3$	54	1·5	Fused Silica	Yuan *et al* (2009)
7	*RT*	10^{13}	–	–	1·5–3	Corning #1737	Takagi *et al* (2005)

voltage of −6·54 V (Hsieh *et al* 2008). On the other hand, active material deposited at 5 Pa (similar pressure) was an enhancement mode TFT with a threshold voltage of +6·2 V (Yuan *et al* 2009).

Thus, it is obvious that the reported TFT characteristics show large variations and all the necessary conditions of device fabrication are not always available to ascertain the reason for the differences. Moreover, since TFT characteristics are affected by multiple factors such as IZGO film properties, choice of structure, and other materials, including the contact, we need to understand the effect of each parameter separately to clearly understand the causes of variations in TFT characteristics. Hence, we also examine the variations in film properties, which supposedly should have been similar.

1.2 *Thin films of IGZO*

Since carrier concentration in IGZO is controlled by the presence of oxygen vacancies, the partial pressure of oxygen (pO_2) during thin film growth plays an important role in modulating the carrier concentration; the carrier concentration can be controlled from 10^{20} cm^{-3} to 10^{13} cm^{-3} in IGZO just by varying the pO_2 from 0·1 Pa to 7 Pa (Takagi *et al* 2005). However, even at a given pressure, the film properties are reported to vary considerably. In table 2, we compare the film properties for IGZO deposited from a target reported to be of composition $InGaZnO_4$. For instance, the films deposited at room temperature at an oxygen partial pressure of 0·1 Pa showed a variation in carrier concentration from 5×10^{14} cm^{-3} (Yuan *et al* 2009) to 10^{20} cm^{-3}

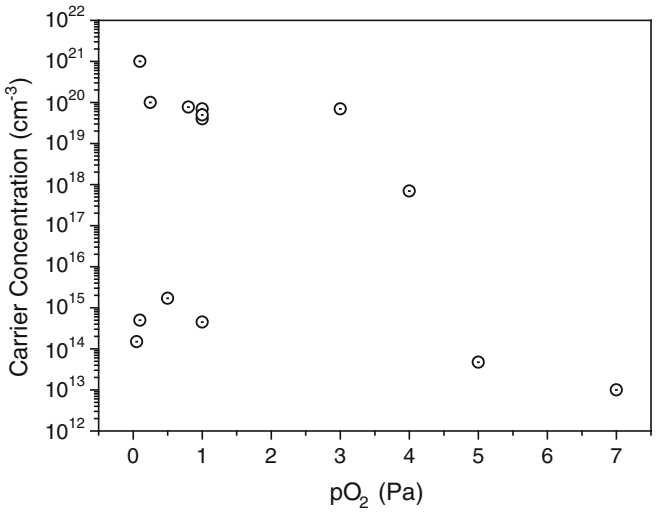

Figure 1. Variation of carrier concentration in thin films of $InGaZnO_4$ deposited by PLD at various pressures of oxygen.

(Takagi *et al* 2005) and at 1 Pa from $4{\cdot}5 \times 10^{14}$ cm^{-3} (Yuan *et al* 2009) to 10^{19} cm^{-3} (Hosono 2006; Kamiya *et al* 2006; Nomura *et al* 2006; Hosono *et al* 2008; Nomura *et al* 2008a, b). The variations in carrier concentration reported for various deposition pressures of oxygen are also compared in figure 1, which depicts an enormous variation in the data. Laser fluence is reported in some cases but nevertheless, it cannot alone explain such large variation in carrier concentration. Earlier, we noted that the hall mobility changed from 0·9 to 9 cm^2/Vs upon changing the laser fluence from 2 to 9 J/cm^2 (Hosono *et al* 2008). However, hall mobility as large as 54 cm^2/Vs has been achieved at a laser fluence of 1·5 J/cm^2 (Yuan *et al* 2009).

The survey above clearly illustrates that even when thin films are deposited under similar conditions, there is a large discrepancy in the properties of thin films especially in terms of carrier concentration. The reason for such a large discrepancy is not known, partly because not all details of thin film fabrication conditions are reported. Thus, in order to understand the TFT performance, we will first have to standardize the film preparation method or establish important parameters that must be reported. Also, since thin film growth requires a target for both PLD and sputter deposition, even the target preparation must also be standardized.

1.3 *Sintering method for $InGaO_3(ZnO)_m$ target*

In 1985, Kimizuka and Mohri reported synthesis of $InGaO_3(ZnO)_{0.5}$ and $InGaO_3(ZnO)_1$ by sintering the oxide powder at 1450°C for 6 days and 1 day, respectively. Prior to sintering, the individual oxides were heated at 1000°C for 1 day in air, then mixed and sealed in an evacuated Pt tube. They synthesized a series of solid solutions of $InGaO_3(ZnO)_m$ at different temperatures of 1150°C (Kimizuka *et al* 1995), 1250°C (Kimizuka *et al* 1995), 1350°C (Nakamura *et al* 1991), 1450°C (Kimizuka *et al* 1988) and 1550°C (Kimizuka *et al* 1995). Table 3 lists the conditions of synthesis of $InGaO_3(ZnO)_m$ solid solutions. The d-spacing and the relative intensities of the powder X-ray diffractions of $InGaO_3(ZnO)_m$ prepared at 1450°C (Kimizuka *et al* 1988) were later communicated to the International Centre for Diffraction Data (ICDD). The important points drawn are: (i) the reaction rate in the formation of $InGaO_3(ZnO)_m$ increases with increasing temperature (Kimizuka *et al* 1995), (ii) mixing the starting oxides in molar ratio of 1:1:n::In_2O_3:Ga_2O_3:ZnO with odd values of n and $n \geq 3$ results in the formation of two phases with 1:1:$n-1$ and 1:1:$n+1$ (Kimizuka *et al* 1995). If n is even, single phase is attained, and (iii) the reaction rate in forming $InGaO_3(ZnO)_m$ gets slower with increasing m (Nakamura *et al* 1991).

The literature on IGZO TFTs rarely describes the nature of targets for sputtering or PLD; the composition of the films is assumed in most cases. Of course, we know that target

Table 3. Conditions of preparation of $InGaO_3(ZnO)_m$.

Ref.	Kimizuka *et al* (1995)	Kimizuka *et al* (1995)	Nakamura *et al* (1991)	Moriga *et al* (1999)	Kimizuka and Mohri (1985)	Kimizuka *et al* (1988)	Kimizuka *et al* (1995)
Phase	Temperature (°C)/time (days)	Temperature (°C)/time (days)	Temperature (°C)/time (days)	Temperature (°C)/time (days)	Temperature (°C)/time (days)	Temperature (°C)/time (days)	Temperature (°C)/time (days)
$InGaO_3(ZnO)_1$	1150/7	1250/7	1350/3 + 3	1400/3	1450/1	1450/1	1550/3
$InGaO_3(ZnO)_2$	1150/7		1350/3 + 4	1400/3		1300/5	1550/3
$InGaO_3(ZnO)_3$	1150/7		1350/4	1400/3		1450/4	1550/3
$InGaO_3(ZnO)_4$	1150/7	1250/7	1350/3			1450/6	1550/3
$InGaO_3(ZnO)_5$	1150/7 + 9	1250/7	1350/3			1450/8	1550/3

(Note: $(s + t)$ days means the following: After heating a specimen for s days, it was rapidly cooled to room temperature. Subsequently, the specimen was carefully crushed in an agate mortar under ethyl alcohol and heated for t days again, followed by rapid cooling to room temperature (Kimizuka *et al* 1995)).

composition depends on the ratios when individual powders are mixed before sintering. But, at elevated temperatures of sintering, there is a possibility of preferential loss of Zn, modifying the composition of the target. In this paper, we demonstrate this possibility and accordingly determine the appropriate conditions of sintering. We show that by careful optimization of sintering conditions, one can achieve low temperatures for sintering while avoiding the use of expensive Pt crucibles. Based on this observation, we think, unaccounted loss of Zn during sintering may also be the cause of variations in TFT and film properties reported in literature.

2. Experimental

2.1 *Pellet preparation*

We prepared the IGZO pellet by conventional ceramic synthesis route under different conditions of temperature and time. The starting materials, powders of In_2O_3(99.999%, Sigma Aldrich), Ga_2O_3(99.999%, Alfa Aesar) and ZnO (99.999%, Sigma Aldrich), were mixed together in stoichiometric proportions in an agate mortar and pestle for about 30 min and then pressed in a steel die to form a green pellet of dimension, 20 mm in diameter and ∼3 mm in thickness. The green pellets were sintered in air under various conditions of time and temperature. For sintering above 1200°C, the pellet was kept on Pt, while below 1200°C, it was kept on fused silica. In some cases, the pellet was sintered for a specified time, cooled and was followed by regrinding it thoroughly in an agate mortar and pestle. Small amount of 4% wt./vol. polyvinyl-alcohol was added as a binder to the ground powder which was again cold pressed at 2500 psi before re-sintering. In all cases, the rate of heating, from room temperature to the required temperature of sintering was maintained at 2°C/min. After the completion of sintering, the pellet was furnace cooled.

2.2 *Pellet characterization*

Chemical compositions of the sintered pellets were determined by energy dispersive X-ray (EDX) analysis in a SEM. For elemental analysis by EDX, the pellet was kept analysed without Au coating and was analysed for atomic ratios of the elements from secondary electrons. Chemical analysis of the sintered pellets was also carried out with inductively coupled plasma optical emission spectrometry (ICP-OES) technique. The phase(s) of the sintered pellets were determined by X-ray diffraction (XRD) technique. XRD patterns were recorded employing Cu-Kα radiation.

2.3 *Film preparation*

Prior to the film deposition by PLD, the glass substrates were washed in soap solution, followed by ultrasonication in acetone, methanol and DI water for 15 minutes each and then dried. Thin films of $InGaO_3(ZnO)_5$ were deposited on the cleaned glass substrate. A KrF excimer laser (wavelength, 248 nm, pulse frequency, 10 Hz) was employed to ablate the target with an energy density (fluence) of 2 J/cm^2. Target to substrate distance was maintained at 6 cm and a total of 6000 shots were fired. Thin films have been deposited under different conditions of oxygen partial pressure, varying from 0·15 Pa to 5 Pa. The deposition chamber was evacuated to a base pressure of 8×10^{-4} Pa before passing oxygen into the chamber. The partial pressure of oxygen required for the deposition condition was maintained by the use of a mass flow controller.

3. Results and discussion

The oxides, In_2O_3, Ga_2O_3 and ZnO, mixed in a molar ratio of 1:1:10 (atomic ratio, In:Ga:Zn::1:1:5) are sintered at 1450°C and 24 h, consistent with conditions reported by Kimizuka and Mohri (1985). The pellet thus formed was first examined using XRD to verify the crystallinity and the phases present. The XRD pattern obtained from the pellet is depicted in figure 2(a) showing sharp intense peaks clearly implying high degree of crystallinity. However, upon peak matching, we found that the XRD pattern not only contains the peaks arising from newly formed IGZO phase but also peaks of the un-reacted starting powders, as ascertained below.

Prior to XRD analysis of the sintered pellets, the XRD patterns of individual oxides were indexed to ICDD card numbers 06-0416, 41-1103 and 36-1451 for In_2O_3, Ga_2O_3 and ZnO, respectively. Then, first the peaks in XRD pattern for

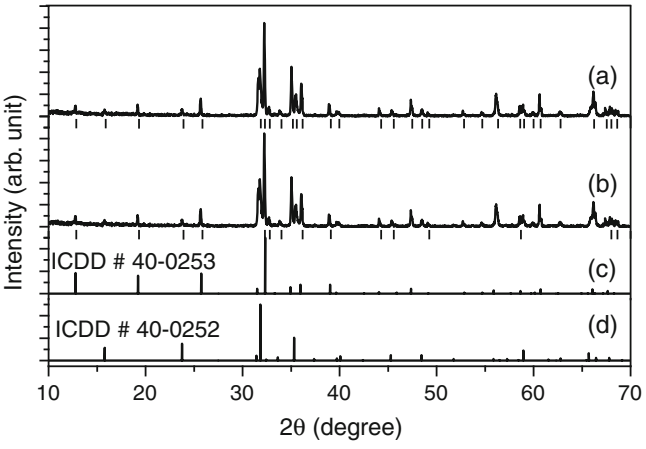

Figure 2. XRD pattern of sample sintered at 1450°C for 24 h in which (**a**) all the peaks are marked for analysis, (**b**) peak positions common to starting oxides (In_2O_3, Ga_2O_3 and ZnO) are removed, (**c**) XRD pattern of $InGaO_3(ZnO)_3$ from ICDD (40-0253), depicting $InGaO_3(ZnO)_3$ as major phase and (**d**) XRD pattern of $InGaO_3(ZnO)_2$ (40-0252) that matches with peaks unidentified by $InGaO_3(ZnO)_3$, indicating its presence.

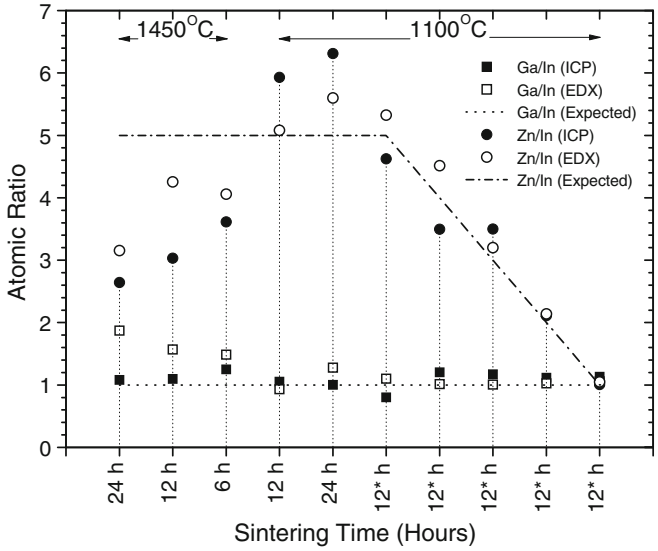

Figure 3. Atomic ratio of Zn/In and Ga/In determined by EDX and ICP-OES techniques for all of the sintered pellets. Note: 12* h represents the pellets sintered for 12 h followed by grinding and re-sintering for another 12 h.

the sintered pellet which may arise from the individual oxides are eliminated, with remaining peak locations depicted as line markers below the diffraction pattern in figure 2(b). Since several major XRD peaks are still available, it is possible to identify the newly formed phase accurately. Accordingly, we determine the new phase to be $InGaO_3(ZnO)_3$ (ICDD card number 40-0253) as shown in figure 2(c). However, a few peaks that still remain unassigned, could be due to $InGaO_3(ZnO)_2$ (ICDD card number 40-0252) as shown in figure 2(d). Finally, the peaks that were removed because of ambiguity with the individual oxides are included back and found to be common with the newly formed phase. This implies that sintering is complete with little or no trace of starting oxides. The same methodology is applied to all XRD analyses reported in this paper.

The phase that forms upon sintering has In:Ga:Zn ratio of 1:1:3, representing loss of Zn during sintering. This loss is also confirmed by EDX measurement for which the atomic ratios are plotted in figure 3 (also see table 4). Zn/In ratio of 3:15 is consistent with the phase measurement, but Ga/In ratio of 1:87 is significantly off. But, much more reliable evidence is provided by a significantly more accurate ICP-OES measurement, also represented in figure 3 and table 4, which would also include any metal associated with amorphous phase, though none are expected at such higher temperatures.

In short, the sintering process that we follow from literature (Kimizuka and Mohri 1985), without the use of sealed Pt tube, is found to result in loss of Zn. Therefore, to preserve the target composition, the sintering process should be modified. The loss of Zn can be prevented in many ways, for example, by sealing the pellet in an appropriate environment during the sintering. Our objective, however, is to develop a simpler process, by modifying the sintering temperature and time conditions, that still conserves the composition of the sintered targets, and which, in turn, would simplify preparation of large size targets (100 mm) for sputtering in larger numbers.

3.1 *Effect of sintering time*

Since sintering for 24 h leads to loss of Zn, the sintering time was lowered. The pellets are again prepared with In_2O_3, Ga_2O_3 and ZnO in a molar ratio of 1:1:10, which should lead to a composition $InGaO_3(ZnO)_5$ in the pellets if no loss of Zn occurs. The XRD patterns of the pellets sintered at 1450°C in figure 4 for all three sintering durations are well matched to a composition $InGaO_3(ZnO)_3$ demonstrating loss of Zn even

Table 4. Conditions of temperature and time for sintering the pellet; the results of phase analysis by XRD and compositional determination by EDX and ICP-OES techniques.

	Sintering		Composition					
			XRD	ICP-OES		EDX		
Targeted value of m in $InGaO_3(ZnO)_m$	Temp. (°C)	Time (h)	m	Ga/In	Zn/In	Ga/In	Zn/In	Comment
5	1450	24	3, 2	1·08	2·64	1·87	3·15	Loss of ZnO
5	1450	12	3	1·10	3·03	1·57	4·25	Loss of ZnO
5	1450	6	3	1·25	3·61	1·49	4·06	Loss of ZnO
5	1100	12	5	1·06	5·93	0·93	5·08	Poor phase
5	1100	24	5	1·00	6·31	1·28	5·60	Poor phase
5	1100	12 + 12	5	0·71	4·79	1·10	5·32	Good
4	1100	12 + 12	4	1·20	3·50	1·02	4·52	Good
3	1100	12 + 12	3	1·17	3·50	1·01	3·20	Good
2	1100	12 + 12	2	1·12	2·11	1·03	2·14	Good
1	1100	12 + 12	1	1·13	1·01	1·06	1·05	Good

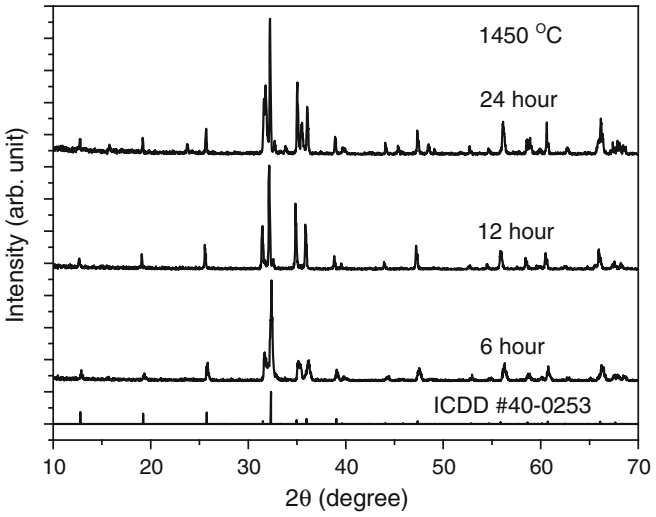

Figure 4. XRD pattern of samples sintered at 1450°C for 24 h, 12 h and 6 h with the starting composition of powders in In:Ga:Zn::1:1:5, which after sintering matches with In:Ga:Zn::1:1:3 suggesting loss of Zn.

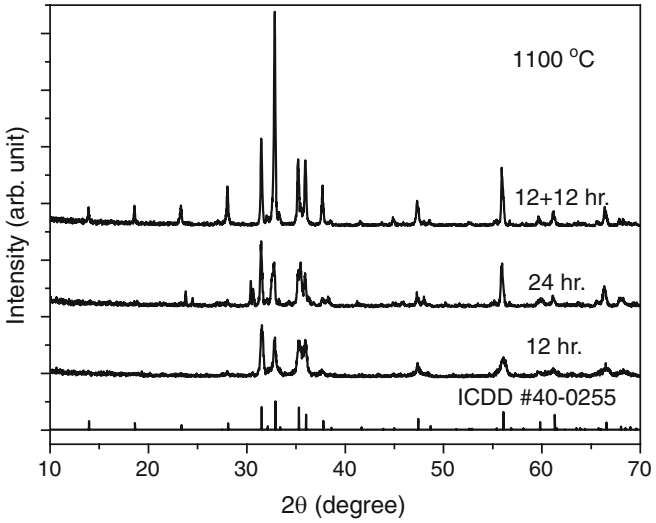

Figure 5. XRD pattern of samples sintered at 1100°C for 12 h, 24 h and 12 h followed by re-sintering for another 12 h after homogenization (labeled as 12 + 12 h). All of the samples show expected final phase of $InGaO_3(ZnO)_5$.

for reduced sintering time of 12 and 6 h. Further increase in sintering time beyond 24 h would only increase the Zn loss, as indicated by formation of additional $InGaO_3(ZnO)_2$, though possibly only in small amounts. The loss of Zn is also validated by EDX and ICP measurements (see figure 3, table 4). Instead of further lowering the sintering time, which may result in loss of control and reproducibility, it would be better to lower the sintering temperature.

3.2 *Effect of sintering temperature*

As it has been observed that sintering at 1450°C causes loss of Zn, we lowered the sintering temperature to 1100°C. The XRD pattern for pellet sintered at this temperature for 12 and 24 h are shown in figure 5, which, for both cases, is indexed to a phase of target composition, i.e. $InGaO_3(ZnO)_5$. Correspondingly, EDX and ICP measurements also confirm retention of Zn in the pellet at this sintering temperature for both 12 and 24 h of sintering and indicating that all metal oxides are locked in a single phase. It may also be noted that not only should the pellet retain its composition consistent with the starting ratio of individual oxides, but also the pellet be in a single phase to retain control over deposition fluence during PLD or sputtering. Thus, it is now possible to attain the desired composition in making sputtering and PLD targets for the deposition of IGZO thin films. But, a closer examination of XRD pattern in figure 5 indicates that though the pellets sintered for 12 and 24 h are indexed to $InGaO_3(ZnO)_5$, the low angle peaks expected in this phase just begin to appear after 24 h of sintering implying that crystallinity is not yet perfect. Hence a modified process is designed to obtain a better quality of phase in the pellet.

3.2a *Modified sintering*: The XRD pattern of the pellet sintered for 12 h, as shown in figure 5, exhibits poor phase formation. Increasing the sintering time to 24 h shows only a minor improvement. However, a pellet sintered for 12 h, followed by grinding it thoroughly and re-sintering for another 12 h not only yields the expected phase of $InGaO_3(ZnO)_5$, the low angle XRD peaks also emerge (see label 12 + 12 h in figure 5). The composition of pellets determined by ICP-OES and EDX also confirms composition consistent with single phase obtained by XRD. This also explains the role of the intermediate grinding stage which homogenizes the samples and aids in the final phase formation.

3.3 *Applicability of sintering process for various compositions*

After optimizing to two-stage sintering process at 1100°C, we prepared pellets of composition, $InGaO_3(ZnO)_4$, $InGaO_3(ZnO)_3$, $InGaO_3(ZnO)_2$, $InGaO_3(ZnO)_1$, corresponding to the In:Ga:Zn atomic ratios of 1:1:4, 1:1:3, 1:1:2 and 1:1:1, respectively. We analysed the phase evolution by XRD and elemental composition by ICP-OES and EDX. The XRD patterns for these compositions are shown in figure 6. We observe that in all cases, the XRD pattern is well resolved even in the low angle region. In table 4 (and figure 6), we indicate the value of m (in $InGaO_3(ZnO)_m$), illustrating single phase formation of desired composition, also confirmed

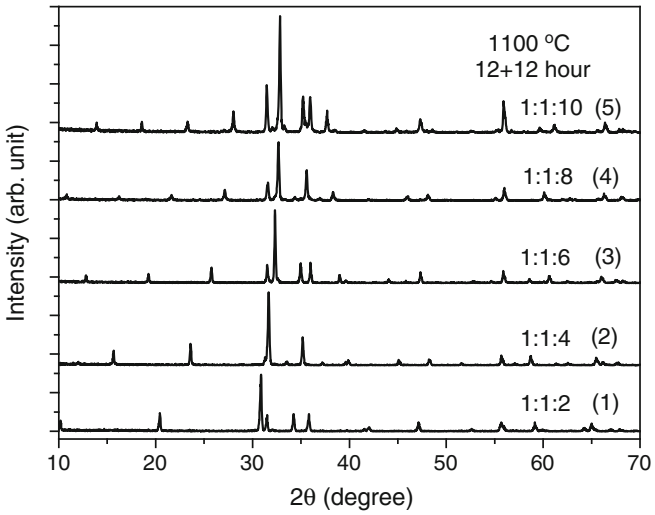

Figure 6. XRD pattern of sintered pellets prepared by re-sintering at 1100°C. Molar ratios of In_2O_3:Ga_2O_3:ZnO and value of m in parenthesis are specified.

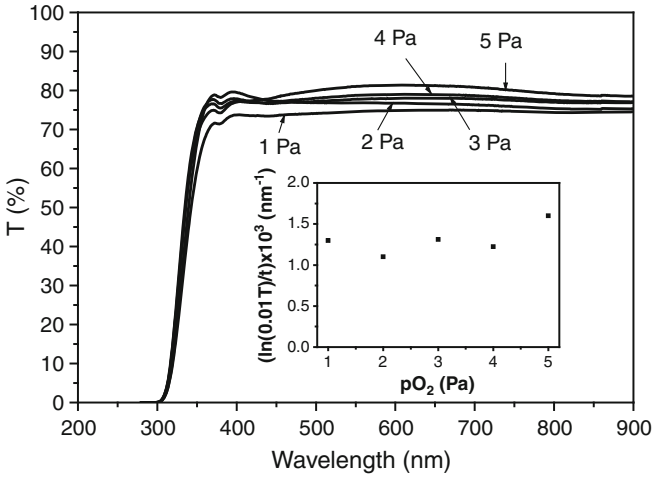

Figure 7. Transmission characteristics of PLD deposited IGZO thin films as a function of oxygen partial pressure (pO_2) during film deposition. Film thicknesses at $pO_2 = 1$, 2, 3, 4 and 5 Pa are 226, 240, 192, 195 and 131 nm, respectively. Inset shows the plot of transparency parameter normalized for film thickness versus pO_2.

by both EDX and ICP-OES. Thus, we explicitly show that the process developed is clearly applicable to a large range of compositions, without any loss of Zn and pellets of single phase.

3.4 *Thin films and transparency characteristics*

In order to assess the quality of the target thus formed, a pellet of composition, $InGaO_3(ZnO)_5$, was used in PLD of films on a cleaned soda lime glass substrate. The films were deposited at different partial pressures of oxygen. We investigated these films by XRD in the 2θ range of 10–50° and found the samples to be amorphous. The films also showed uniform morphology. To investigate quality of films, the transparency of the films on a soda lime glass was compared with an earlier reported data (Suresh *et al* 2008). The transmission of the film on glass deposited at several oxygen pressures, as illustrated in figure 7, is between 75 and 80% in the entire visible region. This result is in accordance with that reported in the literature (Suresh *et al* 2008) for films of same composition. Normally, it is also possible to determine the optical bandgap from the transmission data, but that has not been attempted as the film is deposited on soda lime glass which also has transmission cut-off between 300 and 350 nm.

One should note that the thickness of the films in figure 7 varies slightly with change in the oxygen partial pressure. However, in order to eliminate the effect of thickness, in the inset, we have shown a parameter $-\ln(T/100)/t$, where T is % transmission and t the film thickness, as a function of oxygen partial pressure at 555 nm. The figure clearly shows that the transmission does not depend strongly on the oxygen partial pressure in the range investigated.

In summary, the results suggest that the films deposited by the targets made by the process described in this paper are adequate to obtain amorphous IGZO films of smooth morphology and desired optical properties.

4. Conclusions

The devices made with IGZO show a large variance in characteristics, as reported in literature. It is not possible to conclusively ascertain the reasons of this variance and hence it is necessary to standardize the materials and processes right from the stage of fabrication of targets that are used for depositing the films.

In general, IGZO targets are prepared at temperatures >1200°C. Even at those temperatures, heating was carried out for several days. In most reports, sealed Pt tubes were employed during sintering to avoid evaporation. We have devised a simpler fabrication process which avoids the use of sealed Pt tubes. We have established conclusively that, without use of a sealed Pt tube, sintering at 1450°C leads to loss of Zn. This is an important yet one of the unreported features of IGZO processing. Since the published literature in IGZO devices does not always report the method of preparing IGZO targets, it is possible that, inadvertently, the targets used are not of the same composition as it was thought; this could be one possible reason for the observed variance in the film properties and device characteristics reported in literature.

We have shown that IGZO pellets can be successfully prepared without the use of sealed tubes when sintered at a much lower temperature of 1100°C and for a shorter duration. Preparation of IGZO pellets without the use of sealed Pt or quartz tube would considerably simplify the preparation of target for sputtering and PLD, as it would enable the preparation of a large number of targets of large sizes. Moreover,

use of lower temperatures and shorter time would make the process more economical. We also grew thin films of IGZO using the target made using reported synthesis process and found that the films are of acceptable quality.

Finally, it is important that the targets from which the films are made are first evaluated for composition; its lacking, we believe, is a cause of variation in device characteristics reported in literature.

References

Hosono H 2006 *J. Non-Cryst. Solids* **352** 851

Hosono H, Nomura K, Ogo Y, Uruga T and Kamiya T 2008 *J. Non-Cryst. Solids* **354** 2796

Hsieh H-H, Kamiya T, Nomura K, Hosono H and Wu C.-C 2008 *Appl. Phys. Letts.* **92** 133503

Inoue K, Tominaga K, Tsuduki T, Mikawa M and Moriga T 2008 *Vacuum* **83** 552

Jeong J K *et al* 2008 *SID Digest* **39** 1

Kamiya T, Nomura K and Hosono H 2006 *ECS Meeting Abstracts* **602** 1598

Kim G H, Shin H S, Kim K H, Park W J, Choi Y J, Ahn B D and Kim H J 2008 *SID Digest* **39** 1258

Kimizuka N and Mohri T 1985 *J. Solid State Chem.* **60** 382

Kimizuka N, Mohri T, Matsui Y and Siratori K 1988 *J. Solid State Chem.* **74** 98

Kimizuka N, Isobe M and Nakamura M 1995 *J. Solid State Chem.* **116** 170

Koo C Y *et al* 2008 *J. Korean Phys. Soc.* **53** 218

Lee H-N *et al* 2007 *SID Digest* **38** 1826

Lee J-H *et al* 2008 *SID Digest* **39** 625

Moriga T, Kammler D R, Mason T O, Palmer G B and Poeppelmeier K R 1999 *J. Am. Ceram. Soc.* **82** 2705

Nakamura M, Kimizuka N and Mohri T 1991 *J. Solid State Chem.* **93** 298

Nomura K, Ohta H, Ueda K, Kamiya T, Hirano M and Hosono H 2003 *Thin Solid Films* **445** 322

Nomura K, Ohta H, Takagi A, Kamiya T, Hirano M and Hosono H 2004 *Nature* **432** 488

Nomura K, Takagi A, Kamiya T, Ohta H, Hirano M and Hosono H 2006 *Jap. J. Appl. Phys.* **45** 4303

Nomura K, Kamiya T, Ohta H, Shimizu K, Hirano M and Hosono H 2008a *Phys. Status Solidi (a) – Appl. Mater. Sci.* **205** 1910

Nomura K, Kamiya T, Yanagi H, Ikenaga E, Yang K, Kobayashi K, Hirano M and Hosono H 2008b *Appl. Phys. Letts.* **92** 202117

Ohta H, Huang R and Ikuhara Y 2008 *Phys. Status Solidi-Rapid Res. Letts.* **2** 105

Orita M, Ohta H, Hirano M, Narushima S and Hosono H 2001 *Philos. Mag.* **B81** 501

Shimura Y, Nomura K, Yanagi H, Kamiya T, Hirano M and Hosono H 2008 *Thin Solid Films* **516** 5899

Suresh A, Gollakota P, Wellenius P, Dhawan A and Muthu J F 2008 *Thin Solid Films* **516** 1326

Takagi A, Nomura K, Ohta H, Yanag Hi, Kamiya T, Hirano M and Hosono H 2005 *Thin Solid Films* **486** 38

Yuan L, Fang G, Zou X, Huang H, Zou H, Han X, Gao Y, Xu S and Zhao X 2009 *J. Phys. D: Appl. Phys.* **42** 215301